

# WATER ENTRY OF A BODY WHICH MOVES IN MORE THAN SIX DEGREES OF FREEDOM.

Y.-M. SCOLAN<sup>1</sup> AND A. A. KOROBKIN<sup>2</sup>

<sup>1</sup>ENSTA Bretagne, LBMS, Brest, France

<sup>2</sup>School of Mathematics, University of East Anglia, Norwich, NR4 7TJ, UK

Email address for correspondence: yves-marie.scolan@ensta-bretagne.fr

## Abstract

The water entry of a three-dimensional smooth body into initially calm water is examined. The body can move freely in its six degrees of freedom and may also change its shape over time. During the early stage of penetration, the shape of the body is approximated by a surface of double curvature and the radii of curvature may vary over time. Hydrodynamic loads are calculated by the Wagner theory. It is shown that the water entry problem with arbitrary kinematics of the body motion, can be reduced to the vertical entry problem with a modified vertical displacement of the body and an elliptic region of contact between the liquid and the body surface. Low pressure occurrence is determined; this occurrence can precede the appearance of cavitation effects. Hydrodynamic forces are analysed for a rigid ellipsoid entering the water with three degrees of freedom. Experimental results with an oblique impact of elliptic paraboloid confirm the theoretical findings. The theoretical developments are detailed in the present paper, while an application of the model is described in supplementary materials.

**keywords:** Water impact, three-dimensional flow, free body motion, hydrodynamic loads.

## 1 Introduction

We consider a three-dimensional object with a smooth surface, such as the bow part of a ship hull or the fuselage of an aircraft, approaching the water surface after lifting off or arriving from the atmosphere and penetrating the liquid free surface. The body motion can be computed only by numerical means by taking into account the large displacements of the body, the cavity formation behind the body and the viscous forces acting on the body surface. This problem was studied by [Kleefsman *et al.*(2005)], [Maruzewski *et al.*(2010)], [Tassin *et al.*(2013)], [ Yang & Qiu(2012)] among others. The early stage of water entry, when the wetted surface is in rapid expansion, is difficult to capture numerically but this is the stage during which the hydrodynamic loads acting on the body are very high and may affect the body motions even for longer times.

We focus on the initial stage of the three-dimensional motion of a free body just after the time instant,  $t = 0$ , at which the body touches the water surface at a single point. We consider bodies whose dimensions are of the order of few metres, such as the fuselage of an aircraft or the bow part of a ship hull. For the water entry of such shapes the following assumptions are usually made : i) the viscous effects are neglected since neither a boundary layer nor a separated flow has time enough to develop, ii) the surface tension effects are not taken into account since the local curvature of the free surface is very small (except at the jet root), and iii) the acceleration of the fluid particles exceeds the acceleration of gravity. Those are the reasons for which neither Reynolds nor Froude and Weber numbers are included in the present problem.

In the present analysis, the liquid is assumed to be incompressible and inviscid. The generated flow is irrotational and three-dimensional. Initially,  $t = 0$ , the water surface is flat and horizontal. The body surface in the contact region is approximated by a double curvature surface with two radii of curvature,  $R_x$  and  $R_y$ , which are not necessarily equal and may depend on time  $t$ .

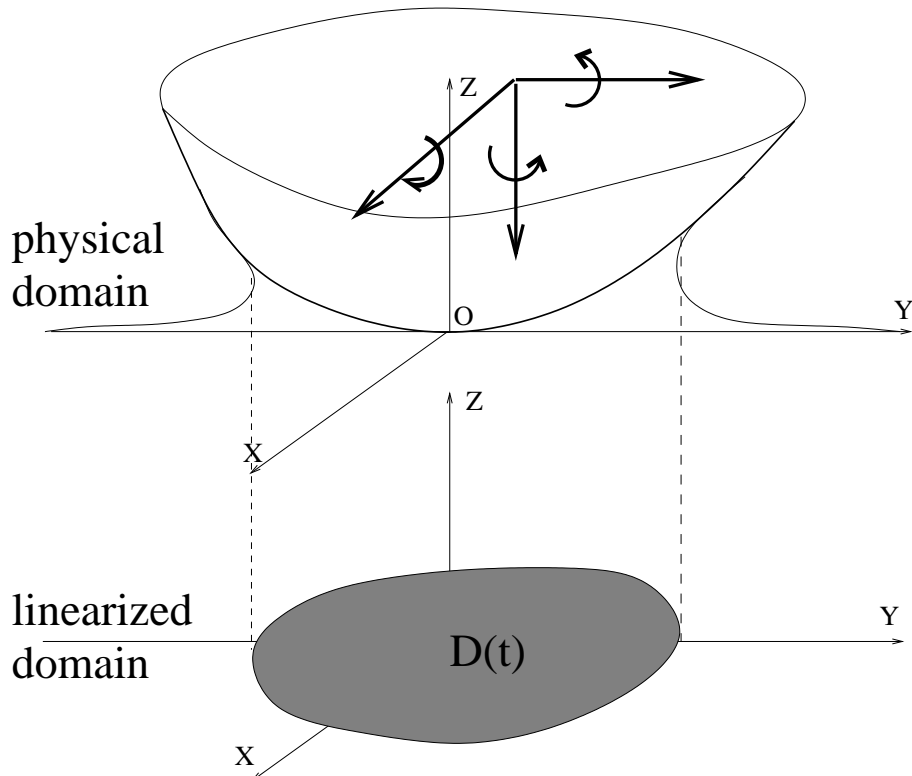


Figure 1: Sketch of a three dimensional body entering an initially flat free surface. The translational and rotational motions (thick arrows) are described in an earth fixed coordinate system. In the linearised domain,  $D(t)$  is the instantaneous expanding wetted surface. This is the projection of the actual wetted surface on the horizontal plane  $(x, y)$ . The contact line is the intersection line between the moving body surface and the deformed free surface in both physical and linearized domain.

Under the assumption of large curvature radii compared to the penetration depth, the resulting boundary-value problem is known as the Wagner entry problem (see [Wagner(1932)]) or "flat-disk approximation" or Wagner's approach. This three-dimensional problem was studied in the past for the standard case of the vertical entry of an elliptic paraboloid (see [Scolan & Korobkin(2001), Korobkin(2002), Scolan & Korobkin(2003), Korobkin & Scolan(2006)]). Note that the Wagner theory assumes small deadrise angles and the wetted area, which expands in all directions over time. For more complex body motions, the oblique impact of an axisymmetric body was studied in [Moore *et al.*(2012)] and the oblique impact of an elliptic paraboloid in [Scolan & Korobkin(2012)]. The present paper aims at generalizing the entry of a smooth three-dimensional body that moves in all possible DoF and changes its shape over time as well. We are unaware of results by others dealing with such complex motions of the body entering water and the corresponding three-dimensional flows. It is shown in the present paper that angular motions of a body change significantly the hydrodynamic loads and their distributions over the wetted part of the body surface. The pressure distribution is carefully analysed in section 5, the zones of negative loads are identified, and the duration of the Wagner stage is examined.

The physical formulation of the entry problem within the Wagner approach is illustrated in Figure (1). The jet flow originated at the periphery of the wetted part of the body surface is not shown in this Figure. The water entry problem for an arbitrary smooth body is formulated in terms of the

displacement potential  $\phi(x, y, z, t)$  (see [Korobkin(1985), Howison *et al.*(1991)])

$$\begin{cases} \nabla^2\phi = 0 & (z < 0), \\ \phi = 0 & (z = 0, (x, y) \notin D(t)), \\ \phi_{,z} = f(x, y, t) & (z = 0, (x, y) \in D(t)), \\ \phi \rightarrow 0 & (x^2 + y^2 + z^2 \rightarrow \infty), \\ \phi \in C^2(z < 0) \cap C^1(z \leq 0) & . \end{cases} \quad (1)$$

Here the lower half-plane  $z < 0$  corresponds to the flow domain,  $D(t)$  is the contact region between the entering body and the liquid, the rest of the boundary,  $z = 0, (x, y) \notin D(t)$ , corresponds to the liquid free surface. The position of the entering body surface is described by the equation  $z = f(x, y, t)$ . In this paper, the function  $f(x, y, t)$  includes the six degrees of freedom of the rigid body motions and the deformations of the body surface expressed in an earth fixed coordinate system. The last condition in (1) implies that the displacement potential  $\phi$  is a smooth function in the flow region, and is continuous together with its first derivatives  $\phi_{,x}$ ,  $\phi_{,y}$  and  $\phi_{,z}$  up to the boundary including the boundary (see [Korobkin & Pukhnachov(1988)]). The latter condition is equivalent to the Wagner condition (see [Wagner(1932)]) and serves to determine the shape and position of the contact region  $D(t)$ . Note that the time  $t$  is a parameter in this formulation. The problem can be solved at any time instant independently. The derivatives  $\phi_{,x}$ ,  $\phi_{,y}$  and  $\phi_{,z}$  provide the displacements of liquid particles in the corresponding directions.

The function  $f(x, y, t)$  from (1) is determined in §2 for the given motions of a rigid body. The displacement potential  $\phi(x, y, 0, t)$  in the contact region  $D(t)$  and the shape of this region are determined in §3. Hydrodynamic forces and moments acting on the body are calculated in §4. The hydrodynamic pressure distribution is analysed in §5. In §6, we consider the problem of a rigid ellipsoid entering water surface at an angle of attack. The obtained results are summarised and conclusions are drawn in §7.

## 2 Shape function of a body during its impact on the water surface

To determine the function  $f(x, y, t)$  in (1), we consider the equations describing the position of the surface of a moving body by taking into account a possible variation of the body shape over time. Let the surface of the body be described by the equation  $z_1 = F(x_1, y_1, t)$  in the coordinate system moving together with the body and such that the global  $x, y, z$  and local  $x_1, y_1, z_1$  coordinates coincide at the impact instant  $t = 0$ . Here  $F(0, 0, t) = 0$ ,  $F_{,x_1}(0, 0, t) = 0$ ,  $F_{,y_1}(0, 0, t) = 0$ , and  $F(x_1, y_1, t) > 0$ , where  $|x_1| > 0$ ,  $|y_1| > 0$  are small. The body surface,  $z_1 = F(x_1, y_1, t)$ , is hence approximated close to the origin by the Taylor series

$$z_1 = \frac{x_1^2}{2R_x(t)} + \frac{y_1^2}{2R_y(t)} + O(r_1^4/R^3), \quad (2)$$

where  $r_1^2 = x_1^2 + y_1^2$  and  $R$  is an averaged curvature radius. We suppose that  $R_y(t) \geq R_x(t)$  and introduce  $\epsilon = \sqrt{1 - R_x(t)/R_y(t)}$  as the eccentricity of the horizontal,  $z_1 = \text{const}$ , sections of the elliptic paraboloid (2).

The body displacements in  $x$ -,  $y$ - and  $z$ -directions are given by the functions  $x_b(t)$ ,  $y_b(t)$  and  $-h(t)$  respectively. The body also rotates with an angle  $\alpha_x(t)$  around the  $x_1$ -axis (roll angle),  $\alpha_y(t)$  around the  $y_1$ -axis (pitch angle),  $\alpha_z(t)$  around the  $z_1$ -axis (yaw angle). We assume that the displacements  $x_b(t)$ ,  $y_b(t)$ ,  $h(t)$  and the angles  $\alpha_x(t)$ ,  $\alpha_y(t)$ ,  $\alpha_z(t)$  are small and equal to zero at  $t = 0$ . The penetration depth  $h(t)$  is chosen here to characterise the initial stage during which  $h(t)/R_x(t) \ll 1$ . The orders of other displacements and angles will be specified below.

For small angles of rotation the global and local coordinates are related by the following equations

$$x = x_1 + x_b(t) - y_1\alpha_z(t) - z_1\alpha_y(t), \quad (3)$$

$$y = y_1 + y_b(t) + x_1\alpha_z(t) - z_1\alpha_x(t), \quad (4)$$

$$z = z_1 - h(t) + x_1\alpha_y(t) + y_1\alpha_x(t). \quad (5)$$

The linear size of the wetted area is estimated by neglecting all motions except the vertical one and by neglecting the free surface elevation. Within this rough approximation, the wetted area is enclosed by the intersection line between the entering body  $z = x^2/(2R_x(t)) + y^2/(2R_y(t)) - h(t)$  and the plane  $z = 0$ . Therefore,  $x$  and  $y$  in the wetted area are of the order of  $\sqrt{h(t)R_x(t)}$  for small  $h(t)/R_x(t)$ . All terms in equations (3)-(5) are of the same order during the initial stage if  $x_b(t)$  and  $y_b(t)$  are of the order of  $\sqrt{h(t)R_x(t)}$ , and the angles  $\alpha_x(t), \alpha_y(t) = O(\sqrt{h(t)/R_x(t)})$ ,  $\alpha_z(t) = O(1)$  as  $h(t)/R_x(t) \ll 1$ . Note that any yaw angles are allowed but we assume  $\alpha_z(t) \ll 1$  in the next developments, keeping in mind that the duration of the initial stage is small and the yaw angle, as other angles cannot vary significantly during this short period. With these orders of the motions all terms in (5) are of the same order. In (4), all terms are of order of  $O(\sqrt{h(t)R_x(t)})$  except the last term which is of a higher order,  $O(\sqrt{h^3(t)/R_x(t)})$ , and can be neglected in the leading order. A similar analysis applied to (3) finally provides that relations (3)-(5) can be approximated in the leading order by

$$x = x_1 + x_b(t), \quad y = y_1 + y_b(t), \quad z = z_1 - h(t) + x_1\alpha_y(t) + y_1\alpha_x(t). \quad (6)$$

Substituting (6) in (2) and rearranging the terms, we obtain

$$z = \frac{(x - X(t))^2}{2R_x(t)} + \frac{(y - Y(t))^2}{2R_y(t)} - Z(t), \quad (7)$$

where

$$X(t) = x_b(t) - R_x(t)\alpha_y(t), \quad Y(t) = y_b(t) - R_y(t)\alpha_x(t), \quad (8)$$

$$Z(t) = h(t) + \frac{1}{2}[R_y(t)\alpha_x^2(t) + R_x(t)\alpha_y^2(t)]. \quad (9)$$

The right-hand side in (7) provides the function  $f(x, y, t)$  in the formulation (1). Note that the horizontal displacements of the body,  $x_b(t)$  and  $y_b(t)$ , are allowed to be much greater than the vertical displacement  $h(t)$ .

### 3 Displacement potential in the contact region

The expression of the shape function  $f(x, y, t)$  following from equation (9) makes it possible to introduce the self-similar variables  $\lambda, \mu, \nu$  as in [Korobkin(2002)]

$$x = X(t) + B(t)\lambda, \quad y = Y(t) + B(t)\mu, \quad z = B(t)\nu, \quad B(t) = \sqrt{2R_x(t)Z(t)}, \quad (10)$$

and the new potential  $\Phi(\lambda, \mu, \nu)$  by

$$\phi = Z(t)B(t)\Phi(\lambda, \mu, \nu). \quad (11)$$

The boundary-value problem with respect to the new unknown potential  $\Phi$  follows from (1)

$$\left\{ \begin{array}{ll} \nabla^2\Phi = 0 & (\nu < 0), \\ \Phi = 0 & (\nu = 0, \quad (\lambda, \mu) \notin D_\epsilon), \\ \Phi_{,\nu} = \lambda^2 + (1 - \epsilon^2)\mu^2 - 1 & (\nu = 0, \quad (\lambda, \mu) \notin D_\epsilon), \\ \Phi \rightarrow 0 & (\lambda^2 + \mu^2 + \nu^2 \rightarrow \infty), \\ \Phi \in C^2(\nu < 0) \cap C^1(\nu \leq 0). & \end{array} \right. \quad (12)$$

Here  $D_\epsilon$  is the contact region in the stretched variables. Its shape depends on the only parameter  $\epsilon = \sqrt{1 - R_x(t)/R_y(t)}$ . The problem (12) is the same as that for an elliptic paraboloid entering the liquid vertically at constant speed. The solution of the latter problem was well investigated by [Scolan & Korobkin(2001), Korobkin(2002), Scolan & Korobkin(2003), Korobkin(2005)] in the past. It was found that the contact region  $D_\epsilon$  is the ellipse

$$\frac{\lambda^2}{a^2} + \frac{\mu^2}{b^2} \leq 1, \quad (13)$$

where  $a = \sqrt{1 - e^2}b$ ,  $b = \sqrt{3/(2 - e^2 - \epsilon^2)}$  and  $e(\epsilon)$  is the eccentricity of the contact region defined by the equation

$$\epsilon^2 = \frac{2(e^4 - e^2 + 1)E(e)/K(e) - (1 - e^2)(2 - e^2)}{(1 + e^2)E(e)/K(e) + e^2 - 1}, \quad (14)$$

$K(e)$  and  $E(e)$  are the complete elliptic integrals of the first and second kind as defined in [Gradshteyn & Ryzhi]. The displacement potential  $\Phi(\lambda, \mu, 0)$  in the contact region is given by [Korobkin(2002)] in the form

$$\Phi(\lambda, \mu, 0) = -\frac{2a}{3E(e)} \left( 1 - \frac{\lambda^2}{a^2} - \frac{\mu^2}{b^2} \right)^{\frac{3}{2}}. \quad (15)$$

Note that the displacement potential (15) in the stretched coordinates system does not depend on any motions but only on the eccentricity of the body sections. This eccentricity can be a function of time.

The comparison between theoretical and experimental results are illustrated in Figures (2) and (3). We consider the oblique entry of an elliptic paraboloid defined by the constant curvature radii  $R_x = 0.75m$  and  $R_y = 2m$ . The kinematics of the moving (undeformable) body reduce to two translational motions in the plane  $(y, z)$ . The  $y$ -horizontal and vertical velocities are  $\dot{y}_b = 0.59m/s$  and  $\dot{h} = 0.79m/s$  respectively. The expansion of the wetted surface is computed and compared to the observations made during an experimental programme at BGO First (La Seyne/Mer, France) in 2011. This programme is described in [Scolan(2012)]. A submerged camera is placed on the basin floor below the impact point. It records along a vertical axis upwards at a frequency of 200 frames per second. In Figure (2) the periphery of the wetted surface at different time instants is marked by a thick white line. Indeed this line is elliptic and it is not affected by the horizontal motion. The results are collected in figure (3). Since the velocities are constant, it is expected that the lengths of the wetted surface increase as  $\sqrt{t}$ , hence the quantities  $aB/\sqrt{h}$  and  $bB/\sqrt{h}$  are plotted in terms of  $\sqrt{t}$ . The variation is therefore linear. The agreement is satisfactory since the error between experiments and theory is within 10%, even at the initial stage where it is more difficult to detect the contact line accurately. The absolute error  $\Delta a$  of measurement is approximately one third the size of the cell grid ( $0.05m$ ) yielding the highest relative error of 20%. More results are available in [Scolan & Korobkin(2012)]. In particular it is observed that the theory slightly overpredicts the experimental data regarding the size of the wetted surface.

## 4 Hydrodynamic loads and equations of the body motions

Taking into account that the hydrodynamic pressure  $p$ , the velocity potential  $\varphi$  and the displacement potential  $\phi$  as well, are zero on the free surface and at infinity, the expressions of the force  $\vec{F}$  and moment  $\vec{M}$  can reduce to

$$\vec{F}(t) = \frac{d}{dt} \int \int_{\bar{D}(t)} \rho \varphi \vec{n} dS, \quad \vec{M}(t) = \frac{d}{dt} \int \int_{\bar{D}(t)} \rho \varphi (\vec{r} \times \vec{n}) dS, \quad (16)$$

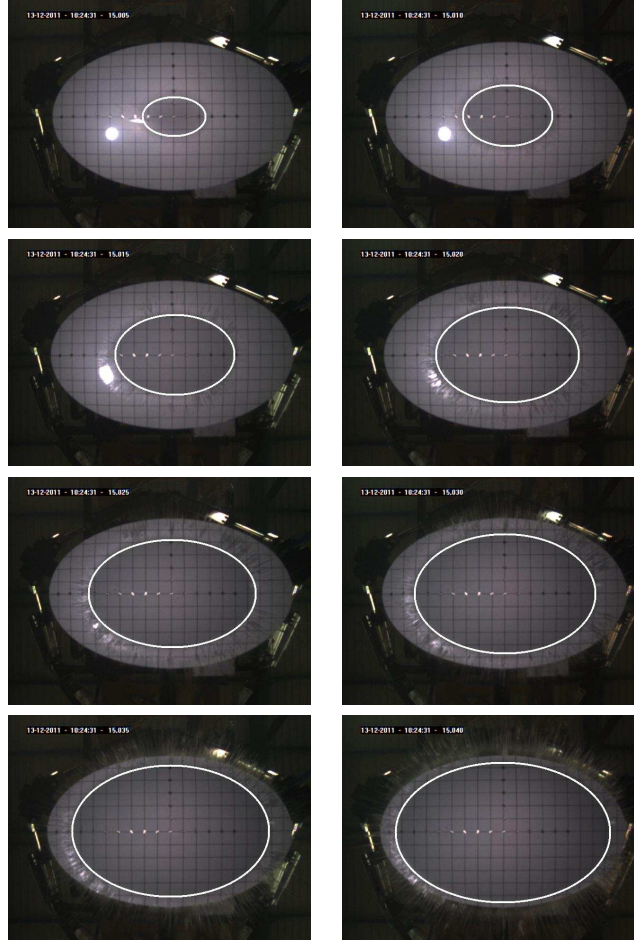


Figure 2: Snapshots of the expanding wetted surface for an oblique entry of elliptic paraboloid defined by  $R_x = 0.75m$ ,  $R_y = 2m$ . The experimental set-up is described in [Scolan(2012)]. The constant vertical velocity and  $y$ -horizontal velocity are  $\dot{h} = 0.79m/s$  and  $\dot{y}_b = 0.59m/s$  respectively. There are no rotations in the experiments. The camera records at 200Hz. The periphery of the wetted area of the body surface at different time instants is marked by a thick white line.

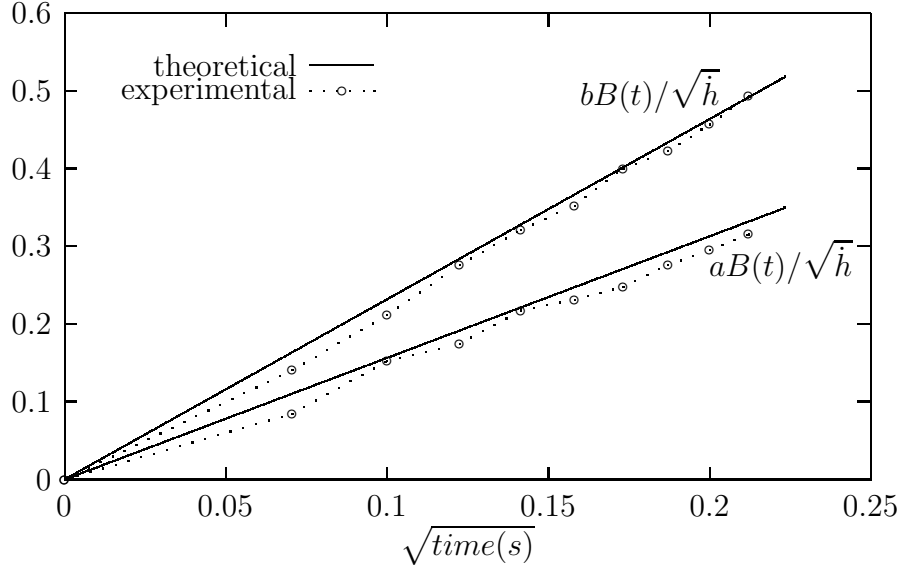


Figure 3: Time variations of the major and minor semi-axes of the elliptic wetted surface, respectively  $bB(t)$  and  $aB(t)$ , divided by  $\sqrt{h}$ . Comparison of experimental data (marks) and theoretical results (solid lines). The vertical velocity and  $y$ -horizontal velocity are  $\dot{h} = 0.79m/s$  and  $\dot{y}_b = 0.59m/s$  respectively.

as shown in [Kochin *et al.*(1964)] for a body moving in unbounded fluid (see pp 394-397). Here  $\rho$  is the density of the liquid. The hydrodynamic moment  $\vec{M}_1(t)$  with respect to the point of the first contact on the body surface,  $\vec{r}_b(t) = (x_b, y_b, -h)$ , is calculated as

$$\vec{M}_1(t) = \vec{M}(t) - \vec{r}_b(t) \times \vec{F}(t), \quad (17)$$

If the position of the entering body is given by the equation  $z = f(x, y, t)$  as in (1), then

$$\vec{r} = (x, y, f(x, y, t)), \quad \vec{n}dS = (f_{,x}, f_{,y}, -1)dxdy. \quad (18)$$

The shape function  $f(x, y, t)$  is given by (7) and the displacement potential  $\phi$  by (11) and (15). It should be noted that  $ff_{,x}, ff_{,y} = O(h\sqrt{h/R_x})$  and  $x, y = O(\sqrt{hR_x})$ . Therefore, the terms  $ff_{,x}$  and  $ff_{,y}$  can be neglected with the relative accuracy  $O(h/R_x)$ . The vertical component of the moment is smaller than two other components and the hydrodynamic loads do not depend on the small yaw angle  $\alpha_z(t)$ . Therefore, the yaw motion can be computed by integration of the corresponding equation, in which the moment is independent of this angle, after other motions have been determined. The equation for the yaw angle is not considered in the following.

Evaluating the integrals in (16), we obtain

$$F_x(t) = -\frac{d}{dt} \left( \frac{\rho A(t) dX}{R_x(t) dt} \right), \quad F_y(t) = -\frac{d}{dt} \left( \frac{\rho A(t) dY}{R_y(t) dt} \right), \quad F_z(t) = \frac{d^2}{dt^2} (\rho A(t)), \quad (19)$$

$$M_x(t) = \frac{d^2}{dt^2} (\rho A(t) Y(t)), \quad M_y(t) = -\frac{d^2}{dt^2} (\rho A(t) X(t)), \quad (20)$$

$$A(t) = -\int \int_{D(t)} \phi(x, y, 0, t) dx dy = N(\epsilon) Z^{\frac{5}{2}}(t) R_x^{\frac{3}{2}}, \quad N(\epsilon) = \frac{8\sqrt{2}\pi a^2 b}{15E(e)}. \quad (21)$$

Note that  $\epsilon$  in (21) can be a function of time for varying radii of the body curvature. It is important to note that  $F_z(t)$  is independent of the body displacements  $x_b(t)$  and  $y_b(t)$  in horizontal directions. However, the force and the moments are strongly dependent on the angles of the body rotations.

If the body is free to move after impact, then the equations of the body motions read

$$\frac{d}{dt} \left( m(t) \frac{dx_b}{dt} \right) = F_x(t), \quad \frac{d}{dt} \left( m(t) \frac{dy_b}{dt} \right) = F_y(t), \quad -\frac{d}{dt} \left( m(t) \frac{dh}{dt} \right) = F_z(t), \quad (22)$$

$$\frac{d}{dt} \left( J_x(t) \frac{d\alpha_x}{dt} \right) = M_{1x}(t), \quad -\frac{d}{dt} \left( J_y(t) \frac{d\alpha_y}{dt} \right) = M_{1y}(t), \quad (23)$$

where  $m(t)$  is the mass of the body and  $J_x(t)$ ,  $J_y(t)$  are its moments of inertia, which could be functions of time if the body changes its shape over time. Equations (22) can be integrated once with the result

$$m(t) \frac{dx_b}{dt} = -\frac{\rho A(t)}{R_x(t)} \frac{dX}{dt} + m(0) \dot{x}_b(0), \quad m(t) \frac{dy_b}{dt} = -\frac{\rho A(t)}{R_y(t)} \frac{dY}{dt} + m(0) \dot{y}_b(0), \quad (24)$$

$$m(t) \frac{dh}{dt} + \frac{d(\rho A)}{dt} = m(0) \dot{h}(0). \quad (25)$$

Here  $\dot{x}_b(0)$ ,  $\dot{y}_b(0)$  and  $-\dot{h}(0)$  are the initial velocities of the body motions in  $x$ -,  $y$ - and  $z$ - directions. Equations (24) yield the speeds of the horizontal motions in terms of the angles of rotation, their time derivatives and the vertical displacement  $h(t)$

$$\frac{dx_b}{dt} = \frac{\dot{x}_b(0)m(0)/m(t) + m_x(t)[R_x\alpha_y]_{,t}}{1 + m_x(t)}, \quad \frac{dy_b}{dt} = \frac{\dot{y}_b(0)m(0)/m(t) + m_y(t)[R_y\alpha_x]_{,t}}{1 + m_x(t)}, \quad (26)$$

where

$$m_x(t) = \frac{\rho A(t)}{m(t)R_x(t)}, \quad m_y(t) = \frac{\rho A(t)}{m(t)R_y(t)}. \quad (27)$$

The vertical displacement  $h(t)$  is governed by equation (25) which can be integrated in time if the mass of the body is constant. It is convenient to introduce the length scale

$$L = \left( \frac{m}{\rho N(\epsilon)} \right)^{\frac{2}{3}} \frac{1}{R_x(t)}, \quad (28)$$

and a new non-dimensional displacement  $\tilde{Z} = Z(t)/L$ . Then equation (25) provides

$$\tilde{Z} + \tilde{Z}^{\frac{5}{2}} = \frac{\dot{h}(0)t}{L} + \frac{R_y(t)}{2L} \alpha_x^2 + \frac{R_x(t)}{2L} \alpha_y^2. \quad (29)$$

The nonlinear equation (29) serves to calculate  $\tilde{Z}(t)$  for given angles of rotation  $\alpha_x(t)$  and  $\alpha_y(t)$  at time  $t$ . Note that we did not use equations for the radii of the body curvature. We assume below that the  $R_x(t)$  and  $R_y(t)$  are given functions of time.

An application is described in supplementary material (8). Given the time variations of the 7 variables ( $h$ ,  $R_x$ ,  $R_y$ ,  $\alpha_x$ ,  $\alpha_y$ ,  $x_b$ ,  $y_b$ ) (hence denoted 7 DoF case) which completely define the state of the dynamical system, the expansion of the wetted surface and the time variation of the loads are assessed. The influence of complex kinematics on the loads is also examined for a free drop configuration; in that case the 7 DoF and the single DoF case (pure vertical motion) are compared.

## 5 Pressure distribution

The pressure follows from the linearised Bernoulli equation  $p = -\rho\varphi_{,t} = -\rho\phi_{,t^2}$ , where  $\phi(x, y, 0, t)$  in the wetted area is given by (10), (11) and (15). If we note  $\phi = -G^{3/2}(x, y, t)$ , then  $G$  appears as a polynomial of order two with respect to  $x$  and  $y$  and we can express  $G$  as

$$G(x, y, t) = \sum_{\substack{i+j \leq 2 \\ i, j=0}} \beta_{ij}(t)x^i y^j, \quad (30)$$

where all (non zero) coefficients  $\beta_{ij}$  only depend on time. Then the pressure can be expressed as

$$p = \frac{3\rho}{4\sqrt{G}} \left( 2\ddot{G}G + \dot{G}^2 \right), \quad (31)$$

where overdot stands for time derivative and the expression  $2\ddot{G}G + \dot{G}^2$  is a polynomial of order 4 in  $x$  and  $y$ .

We first examine the behaviour of the pressure close to the contact line, where  $G(x, y, t)$  vanishes and the pressure is approximated by

$$p(x, y, 0, t) \approx \frac{3}{4}\rho \frac{C^{3/2}}{\sqrt{1 - \lambda^2/a^2 - \mu^2/b^2}} \left( \frac{\partial}{\partial t} \left( \frac{\lambda^2}{a^2} + \frac{\mu^2}{b^2} \right) \right)^2. \quad (32)$$

The time derivative in (32) is calculated for fixed  $x$  and  $y$  by taking into account the relations (10) between  $x, y$  and  $\lambda, \mu$ . As also noted by [Moore *et al.*(2012)], this time derivative is proportional to the normal velocity of expansion of the wetted surface and the first time instant  $t^*$ , when this derivative is zero, provides the duration of the Wagner stage of impact. To find  $t^*$  and the place on the expanding contact line, where the derivative is zero at  $t^*$ , we search the minimum of the time derivative in (32). After some manipulations, and assuming that the ratio  $R_x(t)/R_y(t)$  does not depend on time, it is shown that  $t^*$  is obtained from

$$a^2\dot{B}^2(t^*) = \dot{X}^2(t^*) + k^2\dot{Y}^2(t^*). \quad (33)$$

Equation (33) provides the duration of the Wagner stage  $t^*$  for a body whose aspect ratio  $k_\gamma = \sqrt{R_x/R_y}$  is constant and which moves with 5 DoF. Note that the yaw motion can be approximately neglected during the early stage of impact. Under the same assumptions, it is also shown that the pressure vanishes in the direction of the translational motion. The calculations are more complicated for a general case where  $k_\gamma$  is a function of time.

We are concerned in the following with the zones of negative pressure in the contact region. These zones are bounded by the lines  $p(x, y, 0, t) = 0$  which are defined by the equation  $\dot{G}^2 + 2\ddot{G}G = 0$  as follows from (31). In the latter equation, the first term is positive and  $G(x, y, t) \geq 0$  in the contact region. Therefore, the negative pressure zone may exist only if  $\ddot{G}(x, y, t) \leq 0$ . Then it would be of interest to determine the roots of the polynomial  $\dot{G}^2 + 2\ddot{G}G$ . In practice it is not an easy task to find the lines  $p = 0$ . On the other hand, provided that the time variations of  $(h, R_x, R_y, \alpha_x, \alpha_y, x_b, y_b)$  are given, the numerical computations of the coefficients  $\beta_{ij}$  and their first and second derivatives in time are rather straightforward. For example, a finite difference scheme is expected to be accurate enough to compute  $\dot{\beta}_{ij}$  and  $\ddot{\beta}_{ij}$  if the time variations of  $(h, R_x, R_y, \alpha_x, \alpha_y, x_b, y_b)$  are regular.

The pressure distribution on the wetted surface is studied below for a rigid three-dimensional body with constant radii of curvature  $R_x$  and  $R_y$ . In this case, the identity holds:  $2Z\dot{B} = \dot{Z}B$  at any time, and  $\dot{G}$  calculated from (30) does not contain polynomials of  $x$  and  $y$  greater than 1. By introducing the change of variables between coordinates systems  $(\lambda, \mu)$ , and  $(\xi, \eta)$  as follows

$$\xi(x, y, t) = \frac{\sqrt{2}}{a} \left( \frac{a^2\dot{B}}{2} + \lambda\dot{X} + k^2\mu\dot{Y} \right), \quad \eta(x, y, t) = \frac{1}{b} \left( \mu\dot{X} - \lambda\dot{Y} \right), \quad (34)$$

we can re-arrange  $2\ddot{G}G + \dot{G}^2$  in equation (31), so that

$$\frac{4p\sqrt{G}}{3\rho H^2} = 2Z \left( 1 - \frac{\lambda^2}{a^2} - \frac{\mu^2}{b^2} \right) G^{(2)} + \frac{4Z^2}{a^2 B^2} \left( \frac{a^2 \dot{B}^2}{2} - \dot{X}^2 - k^2 \dot{Y}^2 + \xi^2 + \eta^2 \right). \quad (35)$$

with

$$G^{(2)} = \left( \frac{a\sqrt{8R_x}}{3E} \right)^{2/3} \left( \ddot{Z} + \frac{2Z}{B} \left( \frac{\lambda \ddot{X}}{a^2} + \frac{\mu \ddot{Y}}{b^2} \right) \right), \quad (36)$$

We can conclude that the second term in (35) is positive in the contact region  $D(t)$  as long as

$$T(t) = \frac{a^2 \dot{B}^2}{2} - \dot{X}^2 - k^2 \dot{Y}^2 > 0. \quad (37)$$

The criterion (37) is quite in line with the results of [Moore *et al.*(2012)] who dealt with the oblique entry of an elliptic paraboloid as well. As soon as the left hand side of equation (37) changes its sign, and provided the body motion is such that  $G^{(2)} = 0$ , the pressure becomes negative in a region which is circular in variables  $(\xi, \eta)$  and starts to increase from  $\xi = 0$  and  $\eta = 0$ . The location of the first point  $(x_o, y_o)$  in the contact region where  $p \leq 0$ , and the time instant of its appearance  $t_o$  are defined by  $\xi(x_o, y_o, t_o) = 0$  and  $\eta(x_o, y_o, t_o) = 0$ , with

$$x_o = X - \frac{\dot{X} a^2 B \dot{B}}{2(\dot{X}^2 + k^2 \dot{Y}^2)}, \quad y_o = Y - \frac{\dot{Y} a^2 B \dot{B}}{2(\dot{X}^2 + k^2 \dot{Y}^2)}, \quad (38)$$

where all quantities are evaluated at time  $t_o$ . Once it happens, the wetted surface where the pressure is negative increases monotonically. The corresponding surface is a circle in the coordinate system  $(\xi, \eta)$ . In the coordinate system  $(x, y)$ , that area is constructed parametrically by inverting the linear system (34) with  $\xi = rT(t) \cos \gamma$  and  $\eta = rT(t) \sin \gamma$ , where  $r \in [0, 1]$  and  $\gamma \in [0, 2\pi]$ .

As an example, we restrict the body kinematics to translational motions in the plane  $(y, z)$  with  $\dot{X} = 0$ . By introducing the non-dimensional measure of time  $\tau = \frac{\dot{Y}}{b\dot{B}}$ , the instant at which the pressure first vanishes in the contact region corresponds to  $\tau = \frac{1}{\sqrt{2}}$  as it follows from equation (37). The expanding elliptic area of negative pressure is enclosed by the curve

$$\frac{x^2}{a^2 B^2} + 2 \frac{(y - Y + \frac{bB}{2\tau})^2}{b^2 B^2} = 1 - \frac{1}{2\tau^2}. \quad (39)$$

The ellipse (39) is centered at a point  $x_e = 0$  and  $y_e = Y - \frac{bB}{2\tau}$ , in the downstream part of the wetted surface with respect to the  $y$  translational motion. The aspect ratio of this ellipse is  $\sqrt{2}k$  and can be greater than 1 if  $R_x/R_y > 0.42$ . Note that the aspect ratio of the contact region (13) is equal to  $k$ . The time  $t^*$  at which the negative pressure zone (39) approaches the contact line (13) corresponds to  $\tau = 1$  *i.e.* when the translational velocity  $\dot{Y}$  becomes equal to the velocity of expansion of the wetted surface  $b\dot{B}$ . The corresponding point of intersection is  $x_i = 0$  and  $y_i = Y - bB$ . The negative pressure area hence extends over half the wetted surface, downstream. At the point of intersection, the radii of curvature (in the horizontal plane) of the two curves, the contact line and the zero pressure line (equation 39), are identical  $bBk^2$ . Therefore the two curves do not intersect elsewhere than at point  $(x_i, y_i)$ .

In supplementary material (8), the evolution of the negative pressure zone is assessed for a more general case. It is shown that the negative pressure surface may expand much faster than the wetted surface itself.

## 6 Oblique impact of an ellipsoid on the flat free surface

This section is motivated by the problem of aircraft landing on the water surface. The fuselage of an aircraft is an elongated structure and hydrodynamic loads acting on it during landing can be described by the strip theory [Tassin *et al.*(2013)]. By "strip theory" we mean a way to construct a three-dimensional flow solution over an elongated body by computing successive twodimensional solutions in cross sections perpendicular to the direction of the maximum elongation of a body. However, at the very beginning of the landing, the contact region of the fuselage is not elongated and the three-dimensional impact theory should be used to describe the loads during this stage.

As an illustration we consider the oblique impact of the ellipsoid

$$\frac{\hat{x}^2}{\hat{a}^2} + \frac{\hat{y}^2}{\hat{b}^2} + \frac{\hat{z}^2}{\hat{c}^2} = 1 \quad (40)$$

on an initially flat water surface  $z = 0$ . In equation (40),  $\hat{x}$ ,  $\hat{y}$  and  $\hat{z}$  are local coordinates with the origin at the centre of the ellipsoid, and  $\hat{a}$ ,  $\hat{b}$  and  $\hat{c}$  are the corresponding semi-axis. Initially, the ellipsoid is above the flat free surface, inclined at an angle  $\alpha_0$  and touches the free surface at the origin of the global coordinate system  $x, y, z$ . Then the body starts to move in the  $(x, z)$  plane with the global coordinates of its centre being  $x_c(t)$  and  $z_c(t)$  and the angle of rotation  $\alpha(t)$ , where  $\alpha(0) = \alpha_0$  and

$$z_c(0) = \sqrt{\hat{c}^2 \cos^2 \alpha_0 + \hat{a}^2 \sin^2 \alpha_0}, \quad x_c(0) = (\hat{a}^2 - \hat{c}^2) \sin \alpha_0 \cos \alpha_0 / z_c(0). \quad (41)$$

In this section, the displacements  $X_c(t) = x_c(t) - x_c(0)$  and  $Z_c(t) = z_c(t) - z_c(0)$ , and the angle  $\alpha(t)$  are assumed to be given functions of time  $t$ . Using the relations

$$\hat{x} = (x - x_c) \cos \alpha + (z - z_c) \sin \alpha, \quad \hat{z} = -(x - x_c) \sin \alpha + (z - z_c) \cos \alpha, \quad \hat{y} = y \quad (42)$$

between the local and global coordinates, equation (40) can be written in the global coordinates and approximated around the point of the first contact,  $x = y = z = 0$ , in a similar way as it has been done in §2 (see Eq. 7). The difference is that now the body motion is described with respect to its centre and the angle of the body rotation is not assumed to be small. The result is

$$z \approx \frac{(x - X(t))^2}{2R_x(t)} + \frac{y^2}{2R_y(t)} - Z(t), \quad (43)$$

where

$$R_x(t) = \hat{A}^3(t)\hat{D}^3(t)\hat{a}^2\hat{c}^2, \quad R_y(t) = \hat{A}(t)\hat{D}(t)\hat{b}^2, \quad X(t) = R_x^2(t)K(t), \quad (44)$$

$$Z(t) = R_x(t)K^2(t) + \hat{D}(t)/\hat{A}(t) - x_c(t)\hat{B}(t)/\hat{A}^2(t) - z_c(t) \quad (45)$$

and

$$\hat{A}(t) = \sqrt{\hat{a}^{-2} \sin^2 \alpha(t) + \hat{c}^{-2} \cos^2 \alpha(t)}, \quad \hat{B}(t) = (\hat{a}^{-2} - \hat{c}^{-2}) \sin \alpha(t) \cos \alpha(t), \quad (46)$$

$$\hat{D}(t) = \sqrt{1 - x_c^2(t)/(\hat{A}\hat{a}\hat{c})^2}, \quad K(t) = \hat{B}(t)/\hat{A}^2(t) + x_c(t)/(\hat{A}^3\hat{D}\hat{a}^2\hat{c}^2). \quad (47)$$

Calculations are performed for the ellipsoid with semi-axis  $\hat{a} = 10\text{m}$ ,  $\hat{b} = 10\text{m}$  and  $\hat{c} = 3\text{m}$ , which is initially inclined at angle  $\alpha_0 = -6^\circ$ . The ellipsoid moves with the horizontal speed 5m/s and penetrates water at speed 1 m/s. The ellipsoid rotates with a constant angular velocity  $\alpha(t) = \alpha_0 + \alpha_v t/T$ , where  $\alpha_v = 6^\circ$  and  $T$  is chosen as 1s. These kinematics are arbitrary but satisfy the basic assumptions of the model.

The positions of three points of the contact line,  $x_m(t)$ ,  $x_p(t)$  and  $y_p(t)$ , in the global coordinates are shown in Figure (4). Here  $x_m(t)$  and  $x_p(t)$  are the maximum and minimum  $x$ - coordinates of

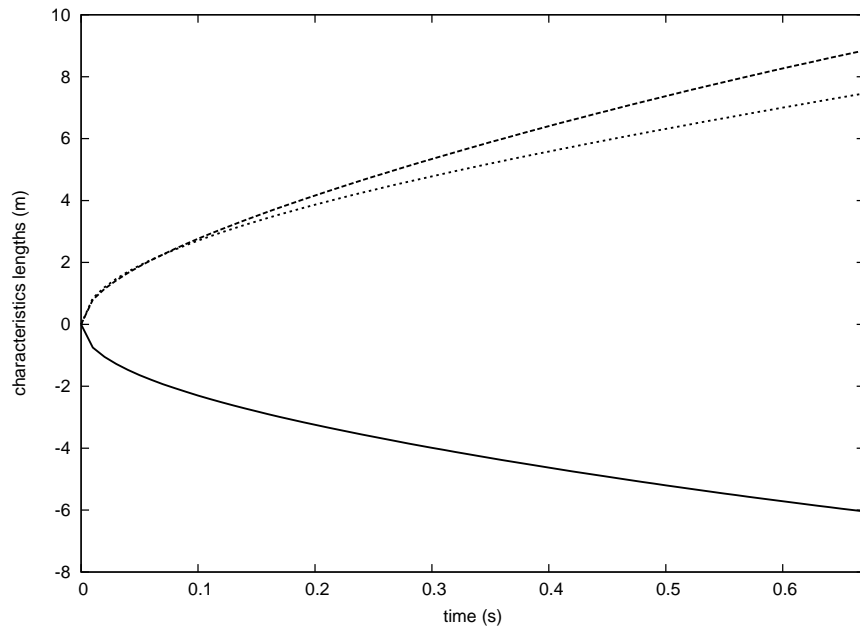


Figure 4: Time variations of positions of 3 points of the contact line: front point  $x_p$  (dashed line), rear point  $x_m$  (solid line) and lateral point  $y_p$  (dotted line).

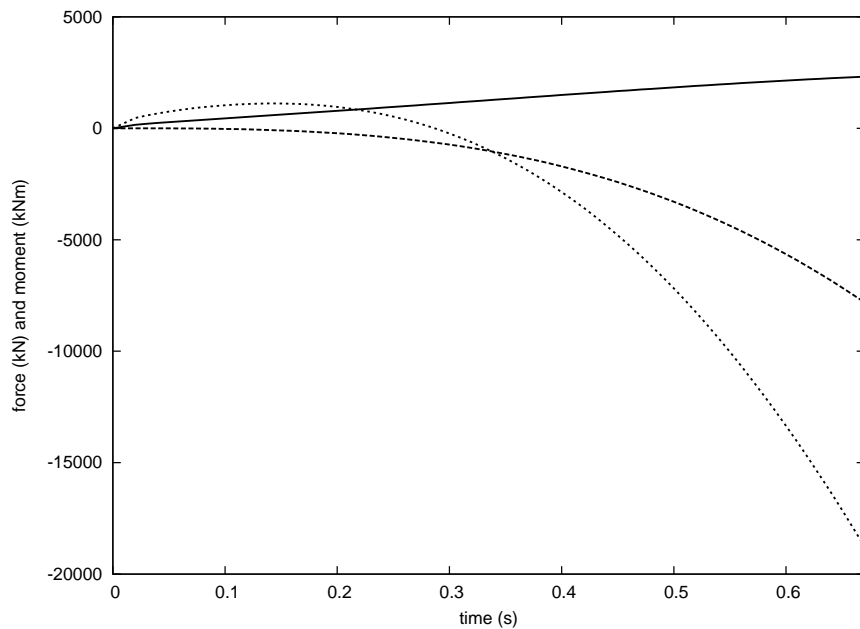


Figure 5: Time variations of the force and moment acting on the ellipsoid. Vertical force  $F_z$  (solid line), horizontal force  $F_x$  (dashed line) and pitch moment  $M_y$  (dotted line).

the contact line, and  $y_p(t)$  is the  $y$ - semi-axis of the contact line. It is observed that the speed of the rear point of the contact line  $\dot{x}_m(t)$  is zero at  $t = 0.67\text{s}$ , which is the duration of the Wagner stage of impact in the case under consideration (see § 5).

Equations (19) - (21), (44) - (45) provide the forces  $F_x(t)$ ,  $F_z(t)$  and the moment  $M_c(t) = z_c F_x - x_c F_z - M_y(t)$  with respect to the centre of the ellipsoid (see Figure 5) during the Wagner stage,  $0 < t < 0.67\text{s}$ . The vertical force  $F_z(t)$  is always positive and almost linear. The horizontal force  $F_x(t)$  is negative and much greater than the vertical force at the end of the Wagner stage. The moment  $M_c(t)$  is positive for  $0 < t < 0.3\text{s}$  while trying to increase the angle of the ellipsoid inclination, and negative after  $t > 0.3\text{s}$  while trying to sink the ellipsoid. In these calculations the motions of the body are prescribed.

## 7 Conclusion

Three-dimensional problem of water impact by a smooth body has been studied. The body moves in six degrees of freedom and changes its shape over time. The liquid flow and the pressure distribution caused by the impact were obtained within the Wagner theory of water impact. Hydrodynamic forces and moments acting on the body were derived in analytical form.

It was shown that water entry of a three-dimensional body moving with six degrees of freedom is rather different from pure vertical entry of the same body. Horizontal displacements of the body and its angular motions may lead to appearance of low-pressure zones in the wetted part of the body surface. These zones may expand in time and approach the periphery of the wetted area, which leads to separation of the liquid surface from the surface of the body at the end of the impact stage of the entry. The present Wagner model fails when cavitation effects appear and when a zone of negative pressure arrives at the contact line. The horizontal velocity of the body can be much higher than its vertical velocity within the present analysis.

The ditching of an aircraft is a particular application of the present theoretical study. The ditching involves mainly the heave, surge and pitch motions of the aircraft. It was shown that the actual shape of the aircraft fuselage can be approximated by an elliptic paraboloid close to the initial contact point and the corresponding shape is characterized by time varying radii of curvature. If the latter are large enough compared to the penetration depth, the Wagner theory provides reliable results in terms of the loads.

Comparisons with experimental results for an oblique entry of an elliptic paraboloid support the present theoretical results for moderate horizontal velocities. In particular it is confirmed that an elliptic paraboloid entering an initially flat free surface with both horizontal and vertical velocities has an expanding wetted surface which is elliptic as well.

### Acknowledgements

The present study is part of the TULCS project which received funding from the European Community's Seventh Framework Programme under grant agreement number FP7-234146. The experimental programme is partly founded by Conseil Général du Var (France). AK acknowledges also the support from EC PF7 project Smart Aircraft in Emergency Situations under the grant agreement number FP7-266172. AK is also thankful to the support by the NICOP research grant "Fundamental Analysis of the Water Exit Problem" N62909-13-1-N274, through Dr. Woei-Min Lin. Any opinions, findings, and conclusions or recommendations expressed in this material are those of the authors and do not necessarily reflect the views of the Office of Naval Research.

# References

- [Gradshteyn & Ryzhik (1994)] GRADSHTEYN, I.S. & RYZHIK, I.M. 1994 Tables of integrals 5<sup>th</sup> edition, Academic Press, 1204pp.
- [Howison *et al.*(1991)] HOWISON, S. D., OCKENDON, J. R. & WILSON, S. K. 1991 Incompressible water-entry problems at small deadrise angles. *J. Fluid Mech.* , **222**, 215-230.
- [von Karman(1929)] VON KARMAN, T. 1929 The impact of seaplane floats during landing. *Technical Notes NASA*, **321**.
- [Kleefsman *et al.*(2005)] KLEEFSMAN, K. M. T., FEKKEN, G., VELDMAN, A. E. P., IWANOWSKI, B., & BUCHNER, B. 2005 A volume-of-fluid based simulation method for wave impact problems. *Journal of Computational Physics*, **206**(1), 363-393.
- [Kochin *et al.*(1964)] KOCHIN, N.E., KIBEL, I.A., & ROZE, N.V., 1964 Theoretical Hydromechanics. *Intersciences Publishers*.
- [Korobkin(1985)] KOROBKIN, A.A. 1985 Initial asymptotics in the problem of blunt body entrance into liquid. *Ph.D thesis*, Lavrentyev Institute of Hydrodynamics.
- [Korobkin(2002)] KOROBKIN, A. A. 2002 The entry of an elliptical paraboloid into a liquid at variable velocity. *Journal of applied mathematics and mechanics* , **66**(1), 39-48.
- [Korobkin(2005)] KOROBKIN, A. A. 2005 Three-dimensional nonlinear theory of water impact. *In 18th International Congress of Mechanical Engineering, Ouro Preto, MG*.
- [Korobkin(2007)] KOROBKIN, A. A., 2007, Second-order Wagner theory of wave impact. *J. Engng. Math.*, **58**(1-4), 121-139.
- [Korobkin & Pukhnachov(1988)] KOROBKIN, A. A. & PUKHNACHOV V. V. 1988 Initial stage of water impact. *Ann. Rev. Fluid Mech.*, **20**, 159–185.
- [Korobkin & Scolan(2006)] KOROBKIN, A. A., & SCOLAN, Y. M. 2006 Three-dimensional theory of water impact. Part 2. Linearized Wagner problem. *J. Fluid Mech.*, **549**, 343-374.
- [Korobkin(2013)] KOROBKIN, A. A. 2013 A linearized model of water exit. *J. Fluid Mech.*, **737**, 368-386.
- [Maruzewski *et al.*(2010)] MARUZEWSKI, P., TOUZÉ, D. L., OGER, G., & AVELLAN, F. 2010 SPH high-performance computing simulations of rigid solids impacting the free-surface of water. *Journal of Hydraulic Research*, **48**(S1), 126-134.
- [Molin *et al.*(1996)] MOLIN, B., COINTE, R. & FONTAINE, E. 1996 On energy arguments applied to the slamming force. *Proc. 11th IWWF, Hamburg, Germany*, 162-165.
- [Moore *et al.*(2012)] MOORE, M. R., HOWISON, S. D., OCKENDON, J. R. & OLIVER, J. M. 2012 Three-dimensional oblique water-entry problems at small deadrise angles. *J. Fluid Mech.* , **711** , 259-280.
- [Moore *et al.*(2013)] MOORE, M. R., HOWISON, S. D., OCKENDON, J. R. & OLIVER, J. M. 2013 A note on oblique water-entry. *J. Engng. Math.*, **81**(1), 67-74.
- [Oliver(2007)] OLIVER, J. M., 2007, Second-order Wagner theory for two-dimensional water-entry problems at small deadrise angles. *J. Fluid Mech.*, **572**, 59-85.

- [Scolan & Korobkin(2001)] SCOLAN, Y. M., & KOROBKIN, A. A. 2001 Three-dimensional theory of water impact. Part 1. Inverse Wagner problem. *J. Fluid Mech.*, **440**(1), 293-326.
- [Scolan & Korobkin(2003)] SCOLAN, Y. M., & KOROBKIN, A. A. 2003 Energy distribution from vertical impact of a three-dimensional solid body onto the flat free surface of an ideal fluid. *J. Fluids and Structures*, **17**(2), 275-286.
- [Scolan & Korobkin(2012)] SCOLAN, Y.-M. & KOROBKIN, A. A. 2012 Hydrodynamic impact (Wagner) problem and Galin's theorem. In *Proc. 27th IWWF, Copenhagen, Denmark*, 165-168.
- [Scolan & Korobkin(2012)] SCOLAN, Y.-M. & KOROBKIN, A. A. 2012 Low pressure occurrence during hydrodynamic impact of an elliptic paraboloid entering with arbitrary kinematics. In *Proc. 2nd Int. Conf. on Violent Flows*, 1-8.
- [Scolan(2012)] SCOLAN, Y.-M. 2012 Hydrodynamic loads during impact of a three dimensional body with an arbitrary kinematics (in french). *Proc. 13<sup>th</sup> Journées de l'Hydrodynamique, Chatou, France.*
- [Tassin et al.(2013)] TASSIN, A., PIRO, D. J., KOROBKIN, A. A., MAKI, K. J., & COOKER, M. J. 2013 Two-dimensional water entry and exit of a body whose shape varies in time. *Journal of Fluids and Structures*, **40**, 317-336.
- [Yang & Qiu(2012)] YANG, Q., & QIU, W. 2012 Numerical simulation of water impact for 2D and 3D bodies. *Ocean Engineering*, **43**, 82-89.
- [Wagner(1932)] WAGNER, H. 1932 Über Stoss- und Gleitvorgänge an der Oberfläche von Flüssigkeiten. *ZAMM*, **12** (4), 193-215.

## 8 Supplementary material: application of the model

That supplementary material contains an application of the model presented in the main body of the paper.

The 7 variables  $(h, R_x, R_y, \alpha_x, \alpha_y, x_b, y_b)$  completely define the state of the dynamical system. We consider the impact problem for a three-dimensional body, the radii of curvature of which are given functions of time  $R_x(t) = R_x(0) + \dot{R}_x(0)t$ ,  $R_y(t) = R_y(0) + \dot{R}_y(0)t$ , where  $R_x(0) = 0.75m$ ,  $\dot{R}_x(0) = -4m/s$ ,  $R_y(0) = 2m$  and  $\dot{R}_y(0) = 30m/s$ . The body moves at speeds  $\dot{x}_b(t) = 7m/s$ ,  $\dot{y}_b(t) = 2m/s$ ,  $\dot{h}(t) = 1m/s$  in the  $x$ -,  $y$ - and  $z$ -directions respectively. The angular velocities of the body are  $\dot{\alpha}_x(t) = 1rd/s$ ,  $\dot{\alpha}_y(t) = 2rd/s$ . The aspect ratio  $k_\gamma(t) = \sqrt{R_x(t)/R_y(t)}$  of the horizontal sections of the body and the aspect ratio  $k(t) = a(t)/b(t) = \sqrt{1 - e^2(t)}$  of the wetted surface are shown in Figure (6a) as functions of time. The time simulation runs up to  $t = 0.05s$ . The modified vertical displacement  $Z(t)$  of the body is given by equation (9) and shown in Figure (6b). It is observed that the modified penetration depth  $Z(t)$  is greater than the vertical displacement of the body  $h(t) = \dot{h}(0)t$ . The Wagner line (periphery of the wetted surface) and the Karman line (intersection of the body with the undisturbed free surface) are computed and plotted in the global coordinate system in Figure (7a) for  $0 < t < 0.05s$ . These lines for the vertical entry of the rigid body (1 DoF) are shown in Figure (7b).

As expected, Figures (7) show that the surface made of all the Wagner lines overlaps the surface made of all the Karman lines. The effect of translational motion along the  $x$  and  $y$  axes, and the variations of the curvature radii are noticeable. The configurations of the submerged body and the related free surface deformation are shown in Figure (8). The free surface elevation in Figure (8) is given by [Korobkin & Scolan(2006)]

$$\eta(x, y, t) = -\frac{1}{2\pi} \int \int_{D(t)} \frac{\Delta_2 \phi(x_0, y_0, t) dx_0 dy_0}{\sqrt{(x - x_0)^2 + (y - y_0)^2}}, \quad ((x, y) \in \text{FS}(t)), \quad (48)$$

where  $\Delta_2 \phi$  is the planar Laplacian of the displacement potential in the wetted area. The integration in (48) is performed numerically over the elliptic wetted surface  $D(t)$ . It should be noted that we cannot expect any asymmetries of the free surface elevation around the body from the equation (48). The free surface pattern is only affected by the body rotations through the modified penetration depth  $Z(t)$ , which is always greater than  $h(t)$  (see equation 9). However, it is not affected by the horizontal motions of the body in the Wagner model.

The force and moment components are computed by equations (19) and (20). The time variations of  $(F_x, F_y, F_z, M_x, M_y)$  are plotted in Figure (9) for the simple vertical motion (1 DoF) and for the complex kinematics (7 DoF). Aparametric study of the influence of each degree of freedom (independently of the others) is performed. That study is not detailed here for sake of brevity. It is remarkable that the vertical force is substantially increased compared to the 1 DoF case, mainly due to the increasing curvature radii along the  $y$  direction. On the other hand the horizontal force is comparable to the vertical force even though it increases more slowly with time.

Free-drop penetration is considered next. Only the vertical motion is free while the horizontal motions  $(x_b, y_b)$  are forced. The time variations of the parameters  $(R_x, R_y, \alpha_x, \alpha_y, x_b, y_b)$  are the same as in Figure (6). The vertical kinematics are computed for the pure vertical motion (1 DoF) and for the complex kinematics (7 DoF). The mass of the body is  $m = 10kg$  and its initial velocity is  $\dot{h}(0) = 1m/s$ . Figures (10) show the time variations of the penetration depth, the velocity and the acceleration. The modification of the shape due to the change of the curvature radii is found to be the main reason for the difference in kinematics.

The evolution of the negative pressure zone is illustrated in Figure (11) for a more general case. The body motions and deformation are governed by the same time variations as for Figure (6). The velocities in  $x$ ,  $y$  and  $z$  directions are constant, and the body has angular motions with constant

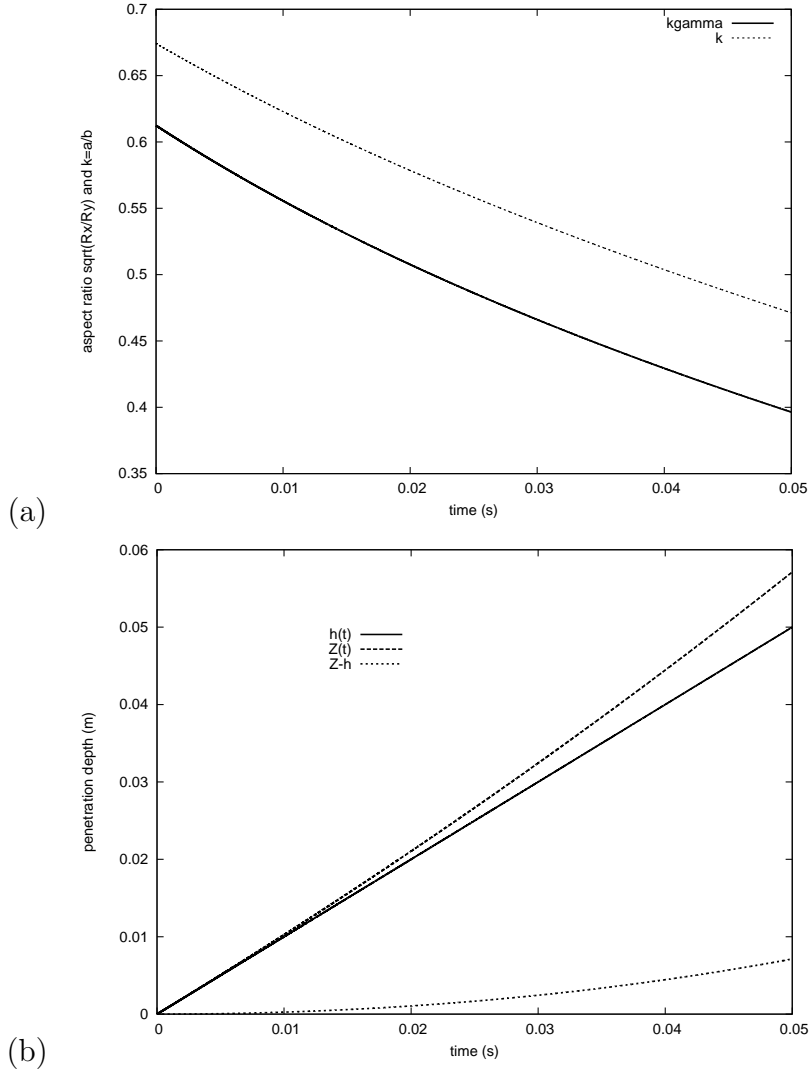
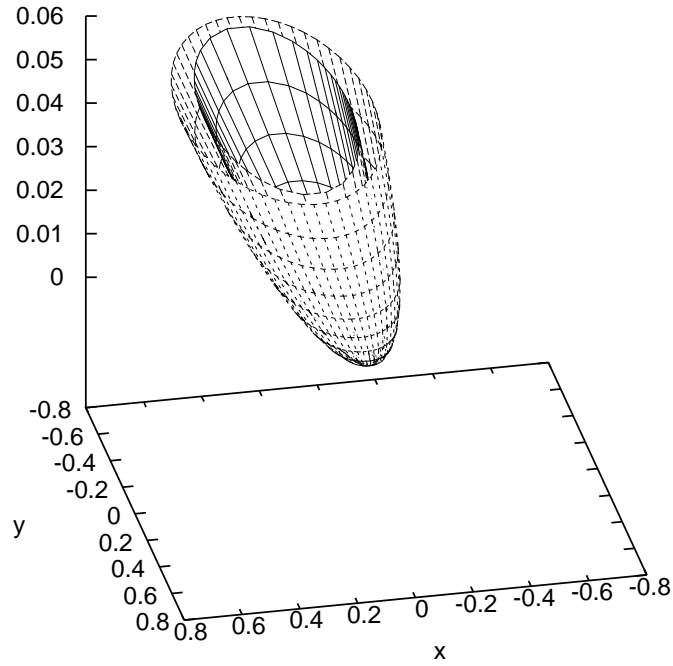
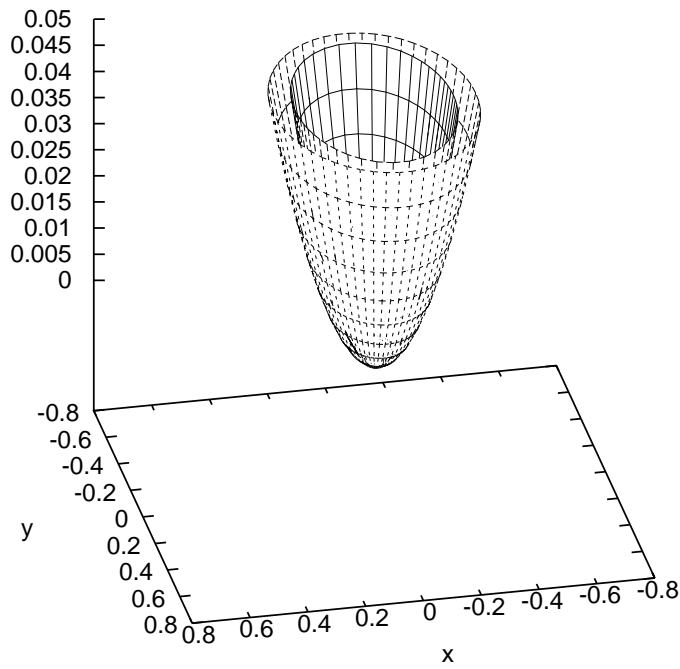


Figure 6: Time variation of (a) the aspect ratios  $k_\gamma = \sqrt{R_x/R_y}$  (solid line) and  $k = a/b$  (dashed line), (b) the penetration depth  $h$  (solid line), the modified penetration depth  $Z$  (dashed line) and the difference  $Z - h$  (dotted line) .

angular velocities as well. Therefore the second derivative of the corrected penetration depth  $Z$  is not zero. It is given by equation (9),  $\ddot{Z}(t) = R_y \dot{\alpha}_x^2 + R_x \dot{\alpha}_y^2$ . In spite of a non-zero contribution of  $G^{(2)}$  (see equation 49) the pressure drops below zero. Figures (11) show the expansion of the negative pressure area as time increases. In the present case, the negative pressure surface expands much faster than the wetted surface itself. It should be noted that this surface mainly migrates towards the negative  $x$  region since the horizontal  $x$ - velocity is greater than the horizontal  $y$ - velocity.

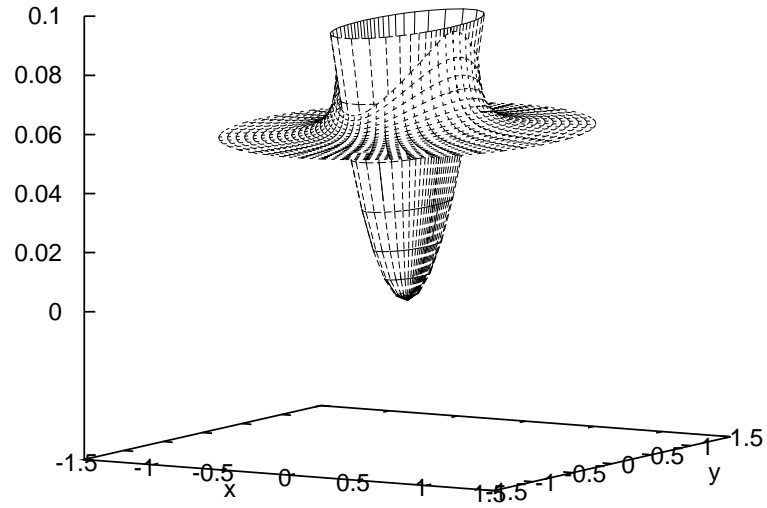


(a)

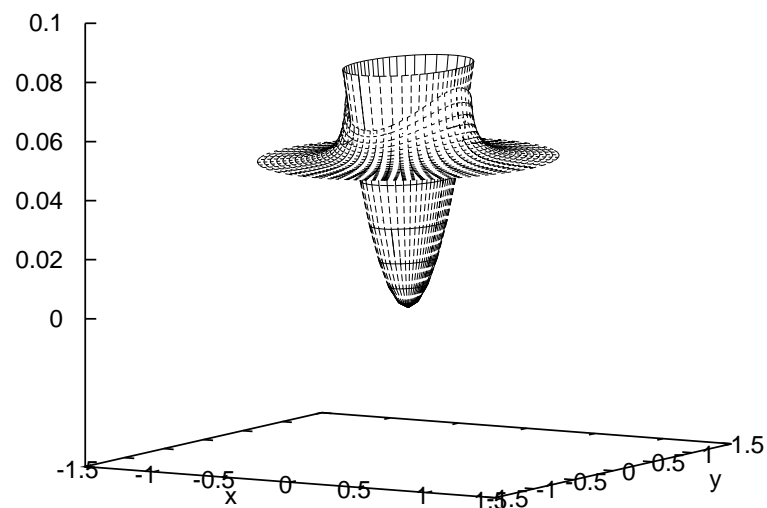


(b)

Figure 7: Wagner line (outer shape) and Karman line (inner shape) computed up to  $t = 0.05s$  during the penetration of the body forced to evolve either with 7 DoF (a) or 1 DoF (b). For 7 DoF, the time variations of parameters ( $R_x, R_y, \alpha_x, \alpha_y, x_b, y_b$ ) are given in the text.



(a)



(b)

Figure 8: Position of the body and corresponding free surface deformation for 7 DoF (a) and 1 DoF (b) at time  $t = 0.05s$ . For 7 DoF, the time variations of parameters  $(R_x, R_y, \alpha_x, \alpha_y, x_b, y_b)$  are given in the text.

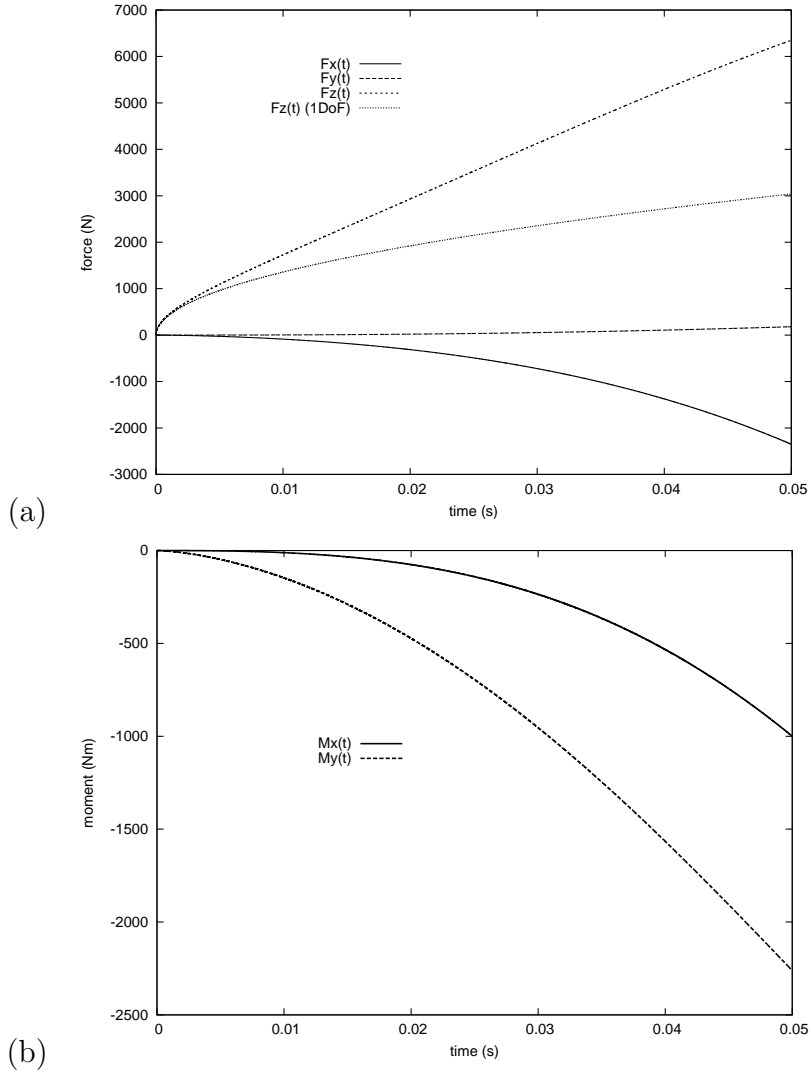


Figure 9: Time variation of (a) horizontal and vertical forces for 7 DoF and 1 DoF, (b) moment around the two horizontal axes. For 7 DoF, the time variations of parameters  $(h, R_x, R_y, \alpha_x, \alpha_y, x_b, y_b)$  are the same as in figure (6).

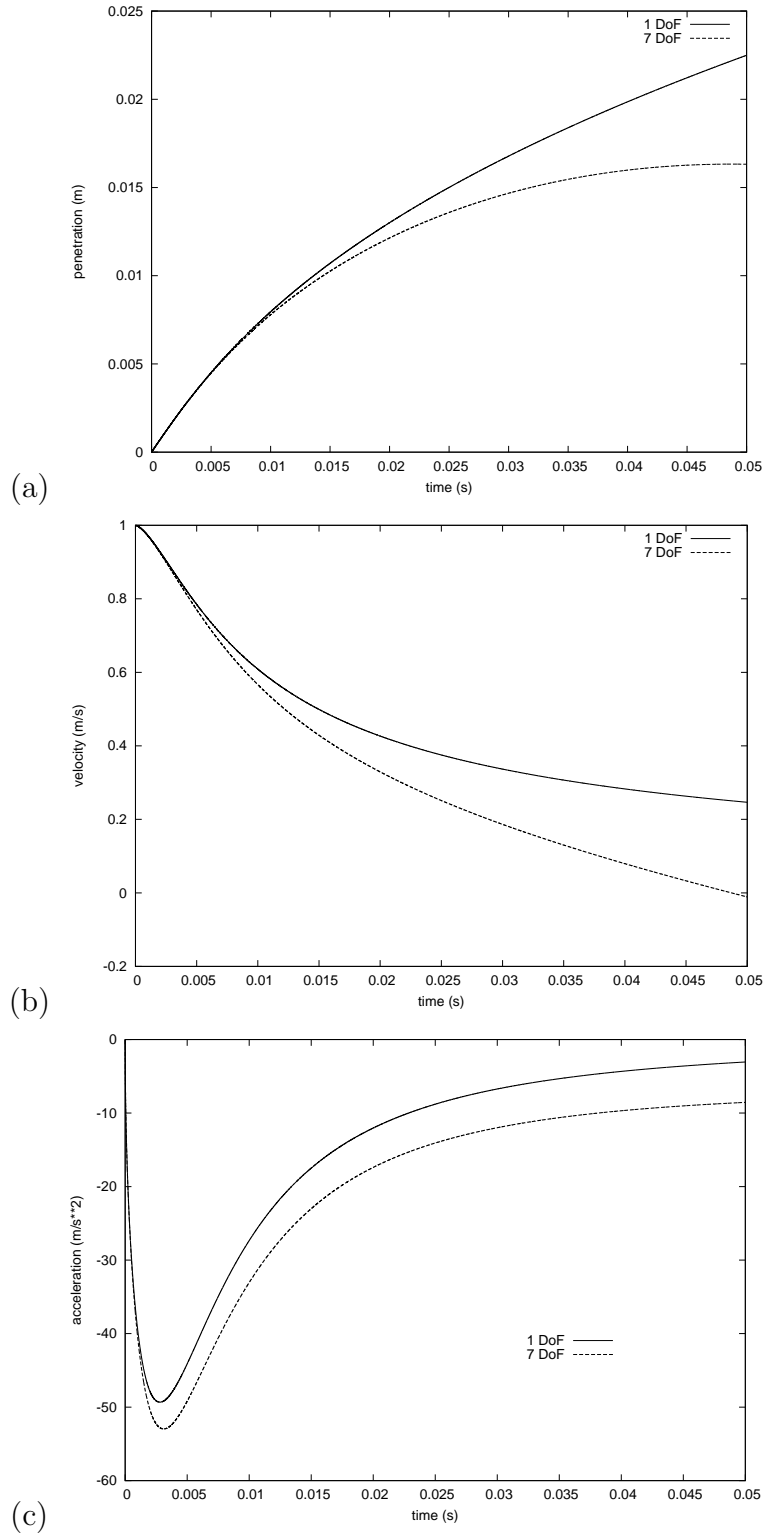


Figure 10: Time variation of (a) the penetration depth, (b) the vertical velocity, (c) the vertical acceleration for 1 DoF (dashed line) and 7DoF (solid line). For 7 DoF, the time variations of parameters  $(h, R_x, R_y, \alpha_x, \alpha_y, x_b, y_b)$  are the same as in figure (6).

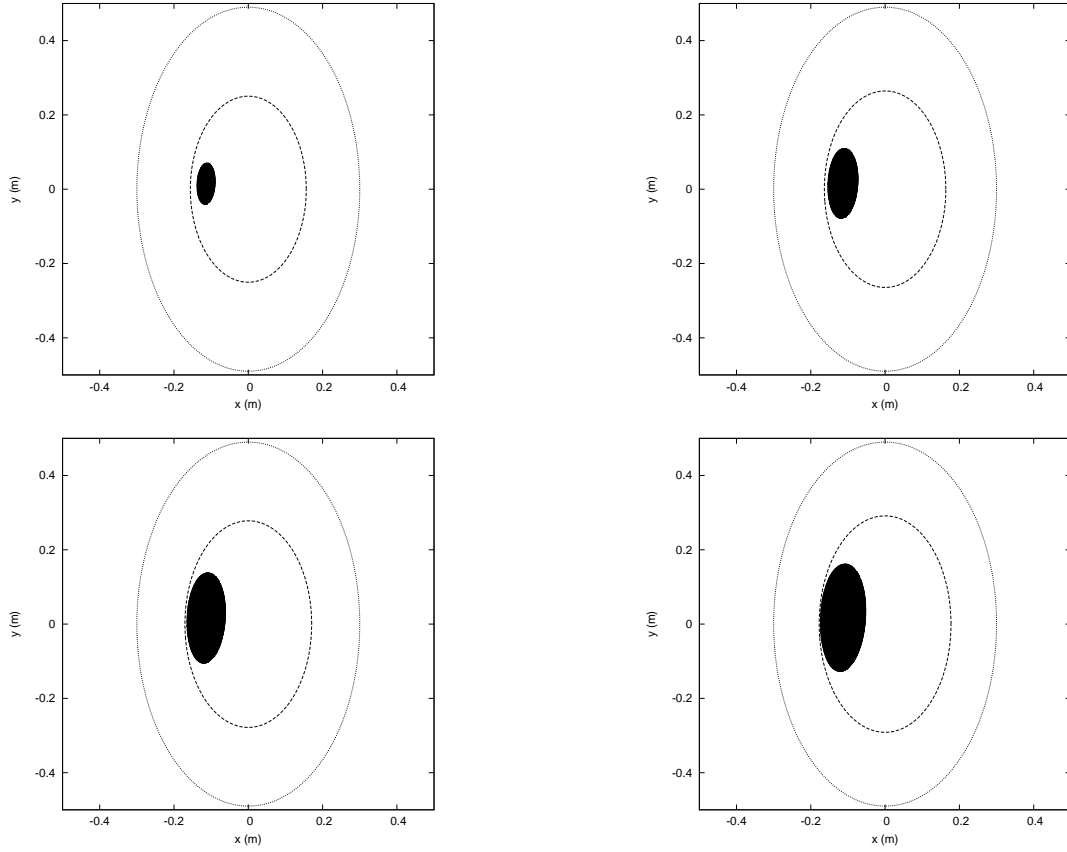


Figure 11: Successive plots of the contact line at time  $t = 0.010s$ ,  $t = 0.011s$ ,  $t = 0.012s$  and  $t = 0.013s$ . The surface of negative pressure is dark and the bigger ellipse gives the finite limit of the elliptic paraboloid. The curves are plotted in the coordinate system centered at  $(X, Y)$ . The time variations of 7 parameters  $(R_x, R_y, \alpha_x, \alpha_y, h, x_b, y_b)$  are the same as for figure (6).